Targeting Serous Epithelial Ovarian Cancer with Designer Zinc Finger Transcription Factors*□S

Haydee Lara[‡§¶1], Yuhua Wang[∥1], Adriana S. Beltran[‡¶¶], Karla Juárez-Moreno[∥∥∥], Xinni Yuan[‡], Sumie Kato[**], Andrea V. Leisewitz[‡‡], Mauricio Cuello Fredes[**], Alexei F. Licea[§], Denise C. Connolly[§§], Leaf Huang[∥], and Pilar Blancafort[‡¶¶2]

From the ‡Department of Pharmacology, the ∥Division of Molecular Pharmaceutics, Eshelman School of Pharmacy, and the ¶¶Lineberger Comprehensive Cancer Center, University of North Carolina, Chapel Hill, North Carolina 27599, §Departmento de Biotecnología Marina, Centro de Investigación Científica y de Educación Superior de Ensenada, Ensenada, México 22860, the ¶Programa de Doctorado en Ecología Molecular y Biotecnología, Universidad Autónoma de Baja California, Ensenada, México 22860, the **Laboratorio de Obstetricia y Ginecología Centro de Investigaciones Médicas, ‡‡Departamento de Hematologia-Oncologia, Facultad de Medicina Pontificia Universidad Católica de Chile 686-3409, the §§Developmental Therapeutics Program, Fox Chase Cancer Center, Philadelphia, Pennsylvania 19111-2497, and ∥∥Centro de Nanociencias y Nanotecnologia Universidad Nacional Autónoma de México, Ensenada, Baja California, México 22860

Background: There is a need for novel targeted therapies for metastatic ovarian cancers.
Results: We reactivated the tumor suppressor *Maspin* in ovarian carcinoma cells by delivering tumor-specific nanoparticles encapsulating a chemically modified ATF-mRNA.
Conclusion: LPR nanoparticles encapsulating the ATF mRNA inhibited ovarian cancer tumor growth in a mouse model.
Significance: We report the first non-viral delivery of an ATF *in vivo* and the discovery of novel anti-metastatic targets for ovarian cancer.

Ovarian cancer is the leading cause of death among gynecological malignancies. It is detected at late stages when the disease is spread through the abdominal cavity in a condition known as peritoneal carcinomatosis. Thus, there is an urgent need to develop novel therapeutic interventions to target advanced stages of ovarian cancer. Mammary serine protease inhibitor (*Maspin*) represents an important metastasis suppressor initially identified in breast cancer. Herein we have generated a sequence-specific zinc finger artificial transcription factor (ATF) to up-regulate the *Maspin* promoter in aggressive ovarian cancer cell lines and to interrogate the therapeutic potential of *Maspin* in ovarian cancer. We found that although *Maspin* was expressed in some primary ovarian tumors, the promoter was epigenetically silenced in cell lines derived from ascites. Transduction of the ATF in MOVCAR 5009 cells derived from ascitic cultures of a Tg*MISIIR-TAg* mouse model of ovarian cancer resulted in tumor cell growth inhibition, impaired cell invasion, and severe disruption of actin cytoskeleton. Systemic delivery of lipid-protamine-RNA nanoparticles encapsulating a chemically modified ATF mRNA resulted in inhibition of ovarian cancer cell growth in nude mice accompanied with *Maspin* re-expression in the treated tumors. Gene expression microarrays of ATF-transduced cells revealed an exceptional specificity for the *Maspin* promoter. These analyses identified novel targets co-regulated with *Maspin* in human short-term cultures derived from ascites, such as *TSPAN12*, that could mediate the anti-metastatic phenotype of the ATF. Our work outlined the first targeted, non-viral delivery of ATFs into tumors with potential clinical applications for metastatic ovarian cancers.

Epithelial ovarian carcinoma (EOC)[3] is the seventh most fatal cancer worldwide and the deadliest malignancy affecting the female reproductive organs (1). Serous ovarian carcinoma (SOC) is the most common form of EOC, comprising 30–70% of the cases (2). SOC is predominantly associated with *p53* mutations, and loss of BRCA1/2 may also predispose to the development of the disease (3, 4). This form is mostly detected at advanced stages, when disease is widely spread and metastasized into the abdomen, in a condition known as peritoneal carcinomatosis. Late diagnosis is explained by the absence of alarming symptoms and the lack of effective screening meth-

[3] The abbreviations used are: EOC, epithelial ovarian carcinoma; SOC, serous ovarian carcinoma; ATF, artificial transcription factor; mATF, murine-specific ATF; GEMM, genetically engineered mouse model; MOVCAR, mouse ovarian carcinoma; ZF, zinc finger; qRT-PCR, quantitative real time-PCR; LPR, liposome protamine RNA; AA, anisamide; EGFP, enhanced GFP; MTT, 3-(4,5-dimethylthiazol-2-yl)-2,5-diphenyltetrazolium bromide; MB, molecular beacon; SR, sigma receptor; TSPAN12, tetraspanin 12; DSPE-PEG,1,2-distearoyl-*sn*-glycero-3-phosphoethanolamine-*N*-[methoxy(polyethylene glycol)-2000].

ods. The lethality of this condition is due not only to late diagnosis but also to transient response to available therapies. Thus, despite achieving optimal de-bulking with surgery and obtaining adequate response to adjuvant chemotherapy, the majority of cases will recur, and patients finally die because of resistant metastatic disease (5–7). Unfortunately, the discovery of biomarkers of metastatic progression and the development of more effective treatments for SOC has been impeded due to our limited understanding of the etiology and progression of the disease.

Genetically engineered mouse models (GEMMs) of epithelial cancers represent powerful model systems as they recapitulate the essential molecular hallmarks of disease development and progression that occur in humans (8). One of those models, the C57BL/6 Tg*MISIIR-TAg* transgenic mouse, develops EOC with metastatic features. Mouse ovarian carcinoma (MOVCAR) cell lines derived from metastatic lesions (ascites) of Tg*MISIIR-TAg* mice recapitulate essential features of SOC, particularly the metastatic potential (9). These cells have the advantage that they can be easily manipulated *in vitro* to elucidate novel biomarkers of metastatic disease and to establish novel delivery systems for therapeutic intervention (9).

Our laboratory has previously described a therapeutic approach to target tumor and metastasis suppressors in cancer cells using arrays of engineered, sequence-specific C_2H_2 zinc finger (ZF) domains (10). Each ZF is composed of a recognition α-helix that binds 3 bp of DNA with high selectivity (11). Six zinc finger (6ZF) arrays read an 18-base pair (18-bp) sequence that is potentially unique in the human genome and provide a high degree of genomic specificity and selectivity (12). Engineering binding specificity is achieved by grafting the α-helical domain of each ZF known to interact with the target DNA triplet (13). We have constructed multimodular 6ZF proteins referred as artificial transcription factors (ATFs), recognizing sequences in targeted promoters with dissociation constants in the picomolar range (10, 13–18). In an ATF, the 6ZF scaffold can be linked to a variety of protein modules to promote transcriptional activation (19–23), repression (24, 25), and more recently, epigenetic editing (26).

We have recently described an ATF (ATF-126) targeting the human mammary serine protease inhibitor (*Maspin*), a tumor and metastasis suppressor gene initially identified in breast cells (27). Although most epithelial cells express high levels of *Maspin*, the promoter is down-regulated by epigenetic mechanisms in several cancers, such as breast (28, 29) and ovarian cancer (30). Endogenous *Maspin* reactivation by ATF-126 was associated with decreased tumor growth by enhancement of apoptosis (10), cell invasion (10), and suppression of metastatic colonization in breast (18) and lung (31) cancer cells. Although most studies have been focused on breast, prostate, and lung cancer, the functional role of *Maspin* as tumor and metastasis suppressor in EOC has not been investigated. Both cytoplasmic and nuclear Maspin expression has been reported in some primary ovarian tumors and cell lines, with nuclear expression being a favorable prognosis factor in ovarian cancer patients (32). Decreased nuclear Maspin expression has been associated with tumor grade and disease progression, suggesting a role of

Maspin silencing in advanced stages of ovarian cancer, potentially in metastatic disease (32–34).

In this manuscript we took advantage of ZF technology to target the endogenous murine *Maspin* promoter in metastatic MOVCAR cell lines to interrogate the functional role and therapeutic potential of *Maspin* in EOC. Delivery of engineered ZF proteins has historically been a major limitation for translational applications, most notably in cancer models. This paper reports the first non-viral delivery of ATF mRNA for future therapeutic treatment of serous epithelial ovarian cancer of advanced stage and potentially for metastatic disease. We also describe a panel of novel targets co-regulated with *Maspin*, which could be used as potential biomarkers for future diagnosis and treatment of metastatic ovarian cancer.

EXPERIMENTAL PROCEDURES

Construction of a Murine-specific ATF Recognizing the Maspin Promoter (mATF)—The murine-specific mATF was designed to recognize an 18-bp duplex 5′-GAAGACCTGG-GTGTGGTC-3′ located at −127 nucleotides upstream the first ATG triplet (translation start site) in the murine *Maspin* promoter (Fig. 1A). The specific ZF coding sequences were generated by overlapping PCR as previously described (10), and the specific α-helical sequences used for the PCR are shown in supplemental Fig. S1. The 6ZF cassette was cloned into the SfiI sites of the retroviral vector pMX-ss-IRES-GFP (10) for endogenous gene regulation studies.

Cell Lines—The T11 cell line was a generous gift from Dr. C. M. Perou (Lineberger Comprehensive Cancer Center, Chapel Hill, NC) (35). Cells derived from the TgMMTV-PyMT were kindly provided by Dr. S. Earp (Lineberger Comprehensive Cancer Center, Chapel Hill, NC). M6CCT and M6C1 breast cell lines from a C3(1)tag mammary mouse model were provided by J. E. Green (NIH, Bethesda, MD) (36). WNT1–3160, WNT1-WG4, BRCA-B1.15, and BRCA-A1.8 cell lines were generously supplied by Dr. L. Varticovski (NIH, Bethesda, MD) and were maintained under culture conditions as previously reported (37–39). MOVCAR 5447, 5612, and 5009 were cultured as described (9).

Retroviral Transduction of mATF in Cancer Cell Lines—Retroviral transduction in the packaging cell line 293TGagPol (ATCC Number CRL-11654) and infection of the host cell lines was performed as described (17) using the retroviral vector pMX-IRES-GFP and the envelope protein plasmid pMDG.1. The cells were infected every 8–12 h for a total of 3 times and collected or fixed 72 h after the first infection for further experiments. The Retro-X Tet-On expression system (catalog number 632104 CloneTech, Mountain View, CA) was used to generate a MOVCAR 5009 stable cell expressing the human *Maspin* cDNA (purchased from Origene, catalogue number SC303231, Rockville, MD) as described (18). To induce *Maspin* cDNA expression, cells were treated for 48 h with doxycycline 100 ng/μl and collected for further experiments. The 293TGagPol cells were grown in DMEM (Sigma) supplemented with 10% of fetal bovine serum (FBS) and antibiotic-antimycotic solution (Sigma).

Treatment of the MOVCAR 5009 Cell Line with Epigenetic Inhibitors—The MOVCAR 5009 cell line was treated with the 5-aza-2′dC DNA-methyltransferase inhibitor and two histone deacetylase inhibitors, suberoylanilide hydroxamic acid and trichostatin A. Cells were treated at saturating concentrations of drugs, as determined empirically for the MOVCAR 5009 cell line: 5 μM 5-aza-2′dC, 10 μM suberoylanilide hydroxamic acid, and 100 nM trichostatin A. All drugs were purchased from Sigma. Cells were plated at a density of 3×10^5 cells in 100-mm plates (Corning, NY) in DMEM media and treated with the corresponding inhibitors during 48 h. Cells were collected, and RNA was extracted with RNeasy Kit (Qiagen) and processed for quantitative real time-PCR (qRT-PCR).

qRT-PCR Assays—RNA from adherent cell cultures and tumor samples were extracted with the RNeasy kit (Qiagen) and reverse-transcribed to cDNA using the High Capacity cDNA reverse transcription kit (Applied Biosystems, Carlsbad, CA). TaqMan Fast Universal Master Mix (Applied Biosystems) and 150 ng of cDNA were used in the PCR reactions. *GAPDH* was used as an endogenous control. Primers used for qRT-PCR studies are shown in supplemental Table S4. The 7500 Software Version 2.0.5. (Applied Biosystems) was used to analyze the data. qRT-PCR was performed in duplicate wells and in three independent experiments. Statistical differences were determined by Student's *t* test considering $p \leq 0.05$ as significant (*), $p \leq 0.01$ as highly significant (**), and $p \leq 0.001$ as extremely significant (***).

Western Blot—Total protein extract was obtained with radio-immune precipitation assay buffer (Sigma R0278). The detection was performed with the Amersham Biosciences ECL detection system (GE Healthcare). A detailed list of the antibodies used in this study, the corresponding suppliers, and the experimental dilutions are shown in supplemental Table S5.

Chromatin Immunoprecipitation (ChIP)—ChIP assay to detect the ATF/polymerase II binding to the murine *Maspin* promoter was performed as described elsewhere (40, 41). Protein-DNA complexes were pulled down with A/G beads (Santa Cruz, sc-2003, Santa Cruz, CA). The beads were washed three times with low salt buffer, three times with high salt buffer, and two times with Tris-EDTA buffer (40, 41). The beads were eluted overnight at 65 °C in elution buffer (Tris-EDTA buffer, 1% SDS, and 2 μl of proteinase K). DNA was isolated by phenol-chloroform extraction. The immunoprecipitated DNA was amplified by PCR using the following primers flanking the mATF binding site in the *Maspin* promoter: 5′-CTGGGTGT-GGTCACAGGTGAGC-3′ and 5′-TCCCTTTGCTTACCTT-GAGTTGC-3. The primers against the murine *GAPDH* promoter were used as controls for the PCR amplifications: 5′-TACTCGCGGCTTTACGGG-3′ and 5′-TGGAACAGGGA-GGAGCAGAGAGCA-3′ (42). The PCR products were loaded in an agarose gel, and the relative -fold enrichment was determined by densitometry (ImageJ, NCBI, Bethesda, MD) and normalized to the input samples.

Immunofluorescence—Cells were seeded in fibronectin-coated coverslips and fixed with 10% formalin-PBS solution at room temperature for 10 min. Cells were permeabilized with 0.5% Triton X, PBS for 15 min at 4 °C, and 4% BSA, PBS was added for overnight blocking at 4 °C. Fibronectin, formalin, and

Triton-X were purchased from Sigma. MOVCAR 5009 cells were transduced with mATF, control, or *Maspin* cDNA and stained for detection of mATF, Maspin, and actin (supplemental Table S5). For immunofluorescence detection of Maspin and tetraspanin 12 (TSPAN12) on epithelial ovarian cancer specimens, paraffin sections (obtained from the UNC Tissue Procurement Core) were deparaffinized, blocked at room temperature with 5% BSA/PBS for 2 h, and incubated with primary antibody overnight at 4 °C. The slides were next washed with 0.03% Tween 20, 1% BSA, PBS and stained with secondary antibodies at room temperature for 1 h. Details regarding the antibody sources and dilutions are specified in supplemental Table S5.

Cell Viability Assay—Cell viability was determined by Cell-Titer Glo assay (Promega, Madison, WI) as described by the manufacturer. Twenty-four hours post-transduction, 1000 cells per well were seeded in 96-well plates, and cell viability was followed every 24 h for a total of 4 days. Statistical differences were determined by Student's *t* test considering $p \leq 0.05$ as significant (*), $p \leq 0.01$ as highly significant (**), and $p \leq 0.001$ as extremely significant (***).

Soft Agar Assay—Cells were collected 72 h post-transduction. Colony formation was assessed using six-well plates (Corning). Five thousand cells per well were seeded on the top layer of 0.3% agar with a 0.6% agar base layer. Plates were incubated for 20 days in a 37 °C incubator with 5% CO_2. Colonies were visualized and counted after a 2-h treatment with a 0.005% crystal violet solution. Cells were seeded in triplicate, and the experiment was repeated three times. Materials were purchased from Sigma unless otherwise stated.

Tumorsphere Assay—Cells were collected 72 h post-transduction and counted. 20,000 cells were seeded in triplicate wells in 6-well plates (low attachment plates, Corning, NY) in spheroid media: HuMEC medium (Invitrogen) containing 20 ng/ml human EGF (BD Biosciences), 1 μg/ml hydrocortisone (Stem Cell Technologies, Vancouver, Canada), insulin 5 μg/ml (Sigma), and $1\times$ B27 (Invitrogen) (43). The plates were incubated at 37 °C in 5% CO_2, and tumorspheres were visualized using a cell culture Leica microscope 10 days after seeding.

Matrigel Invasion Assay—Matrigel Invasion Chambers (BD Biosciences) were used to study cell invasion as previously described (10). Briefly, cells were starved 24 h before the assay, and 1×10^5 cells were seeded in the chambers. 24 h later cells were fixed and stained with hematoxylin and eosin.

Preparation of Modified mRNA—The mATF coding sequence and enhanced green fluorescent protein (EGFP) were cloned into pcDNA 3.1 vector flanked by an untranslated 5′ strong Kozak translational initiation signal and a 3′ α-globin sequence for higher translation efficiency and longer half-life. The untranslated region and gene of interest was amplified by PCR with 5′ primer, CTAGAGAACCCACTGCTTACTGGC-TTATCG, and 3′ primer, [120]TGCGTCGACACTAGTTCTA-GACCCT. The amplicons were used as templates for *in vitro* transcription. Modified mRNA was synthesized with Ambion MEGAScript T7 kit (Invitrogen). A mix of 1.6 μg of purified amplicons, 6 mM 3′-0-Me-m[7]G(5′)ppp(5′)G (New England BioLabs, Ipswitch, MA), 1.5 mM guanosine triphosphate, 7.5 mM adenosine triphosphate, 7.5 mM 5-methylcytidine triphos-

phate, 7.5 mM pseudouridine triphosphate, and 4 μl of T7 enzyme were incubated at 37 °C for 4~6 h. The mRNA was purified with Ambion MEGAclear kit (Invitrogen).

Preparation of Liposome and Liposome Protamine RNA (LPR)—DOTAP (Avanti Polar Lipids, Alabaster, AL) and cholesterol (Sigma) (1:1 mol/mol) were dissolved in chloroform, and the solvent was removed under reduced pressure. The lipid film was hydrated overnight with distilled water to make the final concentration of 10 mM DOTAP and cholesterol. The liposome was sequentially extruded through 400-, 200-, 100-, and 50-nm polycarbonate membranes (Whatman, Piscataway, NJ) to form 80 ~ 100-nm unilamellar liposomes. The LPR core was prepared by mixing 146 μl of solution A (10 μg of mRNA) and 146 μl of solution B (3 μl of 2 mg/ml protamine, 12 μl of 10 mM DOTAP/cholesterol liposome, and 131 μl of distilled water). The resulting solution was incubated at room temperature for 10 min. The pegylation was performed by adding 4 μl of DSPE-PEG$_{2000}$ (Avanti Polar Lipids) (10 mg/ml) and 4 μl of DSPE-PEG$_{2000}$-AA (10 mg/ml) to the LPR core and incubating the mix at 50 °C for 15 min. The DSPE-PEG-AA was synthesized as previously described (44).

In Vitro Transfection of Nanoparticles in MOVCAR 5009 Cells—Ninety-six well plates were seeded with 1×10^4 cells per well. The cells were transfected with either LPR-AA-EGFP or LPR-EGFP nanoparticles equivalent to 0.5 μg of modified mRNA encoding EGFP. Nanoparticles were added to each well in the presence of Opti-MEM medium (Invitrogen) and incubated at 37 °C in 5% CO$_2$. The medium was replaced with complete medium for 4 h post-transfection. The transfection efficiency was determined using a BD FACS Canto Flow Cytometer (BD Biosciences). MOVCAR 5009 cells were transfected with either LPR-AA-mATF or LPR-AA-control. The control refers to the mATF modified mRNA lacking the 5′ cap nucleotide, which inhibits translation. The HA.11 antibody was applied to determine mATF expression by immunofluorescence 24 h after transfection (supplemental Table S5). Transfected cells were processed by MTT cell proliferation assays 2 days post-transfection as described by the manufacturer's instructions (Roche Applied Science). The absorbance was read at 570 nm to determine cell survival.

Molecular Beacon Design and Transfection—The software Beacon Designer (PREMIER Biosoft International, Palo Alto, CA) was employed to design a molecular beacon (MB) probe to hybridize with the mouse *Maspin* mRNA. The MB oligonucleotide sequence 5′-(Texas Red)(C6 amino)-CGCGATCTGTTT-CTGATTCAGGAAATTTCTTCATGATCGCG-(3′BHQ-2)-3′ was synthesized by The Midland Certified Reagent Co. (Midland, TX). LPR nanoparticles loaded with 0.2 μg of MB and 0.8 μg of mATF-mRNA were added into 8-well Lab-Tek Chamber Slides. Twenty-four hours post-transfection cells were examined with fluorescence microscopy observation.

Tumor Reduction Study—4–7-Week-old athymic nude mice (obtained from University of North Carolina animal models core facility) were inoculated with 1×10^7 MOVCAR 5009 cells in the flank. Mice received an intravenous injection (via tail vein) of nanoparticles equivalent to 10 μg of mATF-mRNA/control as a palpable solid tumor was formed (on day 16). Mice received an injection every other day for five times. The

tumor sizes were monitored as an indication of therapeutic effect. Statistical analysis was undertaken using Prism 4.0 GraphPad Software. The tumors were removed and analyzed for expression of the mATF and *Maspin* reactivation by Western blot.

siRNA Transfection—Cells previously transduced with either control or mATF were collected 72 h post-transduction for the siRNA experiment. The murine *Maspin* siRNA and a nonspecific control siRNA targeting luciferase were purchased from Thermo Scientific (Walthman, MA). Transfection was performed using the manufacturer's instructions. Briefly, 1×10^5 cells were plated in 6-well plates, and DharmaFECT 4 was used to transfect the siRNA with a final concentration of 50 nM. Transfected cells were collected 48 h post-transfection and processed for qRT-PCR analysis of *Maspin* and *Tspan12* expression. Data were normalized to control-transfected samples.

Ovarian Cancer Patient-derived Samples—The normal ovary preparation SR06, ovarian primary tumors, and ascites were obtained from the Universidad Católica de Chile with approved Institutional Review Board protocols. These samples were resuspended in Trizol (Invitrogen) and processed for expression analyses. Human ascites (ASC13 to 17) were obtained from University of North Carolina hospitals with approved Institutional Review Board protocols. These cells were grown in RPMI media with 5% FBS in adherent tissue culture plates as described above. Tumor cells were passaged three times in tissue culture dishes and processed for qRT-PCR or Western blot. The epithelial origin of these cells was verified by Western blotting using anti- Pan-Cytokeratin antibodies (supplemental Fig. S4). For the qRT-PCR experiments the samples were analyzed using the GAPDH gene. Two additional endogenous controls recommended for ovarian tumor specimens (the genes glucuronidase β (GUSB) and peptidylprolyl isomerase A (PPIA) (45, 46)) were also used to validate the quantifications.

Gene Expression Microarrays—Total RNA was purified from control and mATF-transduced cells (three biological replicates) as described (18). The mRNA was amplified, labeled, and hybridized as previously described (47) using Agilent mouse 4×180 K oligo microarrays (Agilent Technologies). All microarray data have been deposited in the Gene Expression Omnibus (GEO) data base under the accession numbers: GSM891209, GSM891210, GSM891211, GSM891212, GSM891213, and GSM891214. The probes/genes were filtered by requiring the lowest normalized intensity values to be >10 in both samples and controls. The normalized log2 ratios (Cy5 sample/Cy3 control) of probes mapping to the same gene were averaged to generate independent expression estimates. Statistical analysis of microarray for gene expression data were performed using Significance Analysis of Microarray. Gene ontology (GO) analysis was performed using EASE: the Expression Analysis Systematic Explorer (48).

RESULTS

mATF Binds the Murine Maspin Proximal Promoter and Upregulates Its Expression in a Panel of Cell Lines Derived from GEMMs—To up-regulate the murine *Maspin* promoter, we designed a mATF targeting an 18-bp duplex located ~127 nucleotides upstream the translation start site (Fig. 1*A*). This
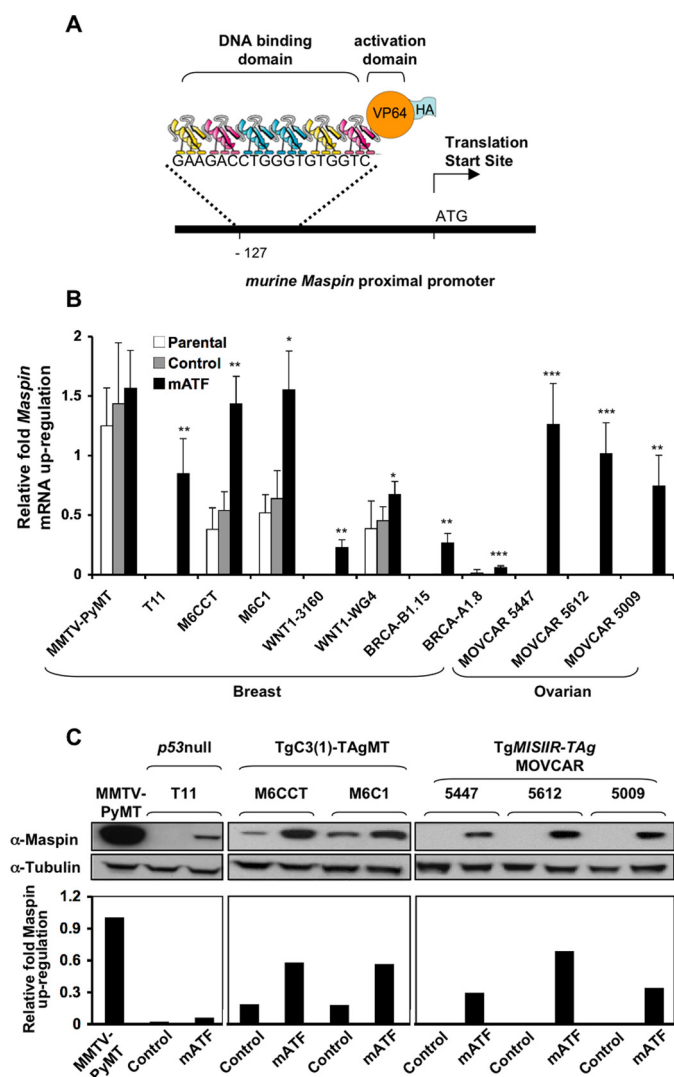
FIGURE 1. **The artificial transcription factor mATF reactivates *Maspin* expression in breast and ovarian cell lines derived from GEMMs.** *A,* shown is a schematic representation of the multidomain structure of the mATF binding the Maspin promoter. The DNA binding domain, composed of six ZF motifs, was designed to bind an 18-bp sequence in the murine *Maspin* proximal promoter at −127 bp upstream the translation start site. The ZF proteins were linked to the VP64 transactivator domain (1). The hemagglutinin (*HA*) tag was engineered at the C terminus of the ZF construct (68). *B,* the mATF up-regulates *Maspin* mRNA expression in breast and ovarian cancer cell lines derived from GEMMs as assessed by qRT-PCR. The mATF and empty vector (control) were retrovirally transduced in the corresponding cell lines. Relative *Maspin* up-regulation in both transduced and parental cell lines are shown in the plot. Data were normalized to the parental MMTV-PYMT cell line. Student's *t* test was used to analyze the differences in gene expression between the parental and the transfected cells (*, $p \leq 0.05$; **, $p \leq 0.01$; ***, $p \leq 0.001$). *C,* shown is an immunoblot analysis of Maspin up-regulation in cell lines derived from GEMMs transduced either with control or mATF. A densitometric analysis of the Western blot is shown. Data were normalized to the MMTV-PyMT cell line. Transgenic mouse strains and cell lines are indicated, and sources are described under "Experimental Procedures."

specific site was chosen because an 18-bp site at the same relative position in the human promoter was successfully targeted by an artificial zinc finger factor, ATF-126 (10). Moreover, because the targeted site was not fully conserved between the murine and the human promoter, the 6ZF helices were re-engineered to regulate the murine counterpart (supplemental Fig. S1).

To have an initial assessment of the potency of the mATF in reactivating *Maspin*, we took advantage of a panel of breast and

ovarian cell lines derived from several GEMMs (Fig. 1, *B* and *C*). We delivered the mATF and an empty vector (control) using the pMX-IRES-GFP retroviral vector system (17). The mATF was able to significantly up-regulate *Maspin* in all the murine cancer cell lines examined carrying low or silenced *Maspin.* The gene expression data were normalized to the parental MMTV-PyMT breast cancer line carrying the highest expression of *Maspin* (Fig. 1*B*). As expected, no significant differences in gene expression were observed between the parental and control-transduced cell lines. We found that although *Maspin* was expressed in some breast cancer cell lines, the gene was silenced in all the ovarian cell lines derived from the Tg*MISIIR-TAg* transgenic mouse. Because of their high invasive potential and their reported phenotypic resemblance to high grade EOC, we focused further experiments using the MOVCAR 5009 cell line. In this background the mATF increased *Maspin* mRNA expression by more than 70,000-fold relative to the parental line, empty vector control cells, or a control vector carrying no ZFs (*VP64-SS* sample, Fig. 2*A*). This regulation required a specific DNA binding as the delivery of a scramble library of ZF proteins linked to VP64 (67) resulted in a significant reduction (more than 3 orders of magnitude) of *Maspin* activation relative to the mATF, indicating that the specific 6ZF domains used for the construction of the protein provided sequence-selectivity (Fig. 2*A*). Interestingly, the reactivation of *Maspin* by the engineered protein was clearly superior to the reactivation of the endogenous gene observed when the parental cell line MOVCAR 5009 was treated with epigenetic inhibitors, such as the DNA methyltransferase inhibitor 5-aza-2′dC (activation of 2564.9-fold over vehicle-control cells) and the histone deacetylase inhibitor trichostatin A (72.96-fold activation over vehicle control-treated cells). Unlike the human *Maspin* promoter (5), the murine counterpart was not significantly up-regulated upon exposure to the histone deacetylase inhibitor suberoylanilide hydroxamic acid. Nevertheless, the clear reactivation of *Maspin* with the methyltransferase inhibitor 5-aza-2′dC suggested that *Maspin* was silenced by promoter methylation in the MOVCAR 5009 cell line. Our results are in agreement with previous mapping of methylated CpG islands by sodium bisulfate sequencing in human ovarian cell lines (30) and suggest that the *Maspin* promoter in metastatic ovarian cell lines is down-regulated by epigenetic mechanisms.

To demonstrate the binding of the mATF to its cognate sequence in the *Maspin* promoter, ChIP assays were performed in the MOVCAR 5009 cells (Fig. 2*B*). Chromatin from empty vector (control) and mATF-transduced cells was isolated, sonicated, and processed for immunoprecipitation assays using an anti-HA antibody to detect the tag engineered at the C terminus of the ZF construct (Fig. 2*B*). The ChIP products were amplified using primers specific for the *Maspin* promoter sequences flanking the mATF site, and the enrichment of the PCR products was evaluated by densitometry. As shown in Fig. 2*B*, mATF-transduced samples, but not controls, yielded the expected *Maspin*-specific 135-bp amplicon, suggesting that the mATF was physically bound to its cognate site in the *Maspin* promoter. Furthermore, when the ChIP assay was performed using an anti-RNA-polymerase II antibody, the immunoprecipitated DNA was enriched in the mATF samples relative to
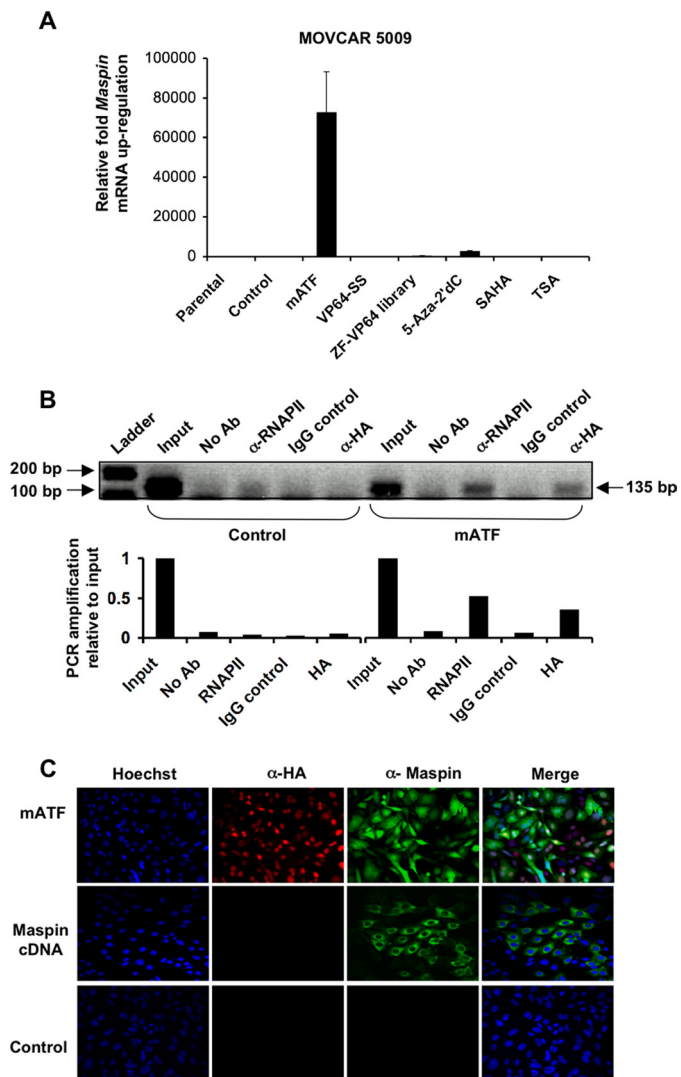
FIGURE 2. **The artificial transcription factor mATF binds the *Maspin* promoter in the MOVCAR 5009 cell line and reactivates silenced *Maspin*.** *A*, retroviral delivery of mATF specifically reactivates *Maspin*, as assessed by qRT-PCR. VP64-SS refers to cells transduced with a vector carrying the transactivator domain but lacking the 6ZFs; *ZF-VP64* indicates a scramble library of 3ZF domains linked to VP64 (69); *Control* refers to empty vector (pMX-IRES-GFP)-transduced cells. The parental cell line was treated with the epigenetic inhibitors: 5-aza-2'dC (5 μM), suberoylanilide hydroxamic acid (10 μM), and trichostatin A (100 nM) at saturating maximum doses. Data were normalized to the parental cell line. *B*, mATF physically binds its targeted site in the *Maspin* promoter. A ChIP assay was performed on the MOVCAR 5009 cell line retrovirally transfected with either control (empty vector) or mATF. α-RNA-polymerase II (*RNAPII*), *IgG Control*, and α-HA antibodies were used to immunoprecipitate the DNA-protein complexes. α-HA facilitated the immunoprecipitation of mATF. Densitometric analysis of the ChIP products loaded on agarose gels after PCR was carried out using the ImageJ software (NCBI, Bethesda, MD). Data were normalized to the signal of the input sample. *Ab*, antibody. *C*, retroviral transduction of mATF in MOVCAR 5009 cells results in reactivation of both cytoplasmic and nuclear Maspin. Immunofluorescence detected the nucleus (Hoechst 2258), the mATF expression (α-HA, *red*), and Maspin (*green*) in MOVCAR 5009 cells transduced with mATF, a Maspin cDNA-expressing retrovirus (18), and an empty retroviral vector or control.
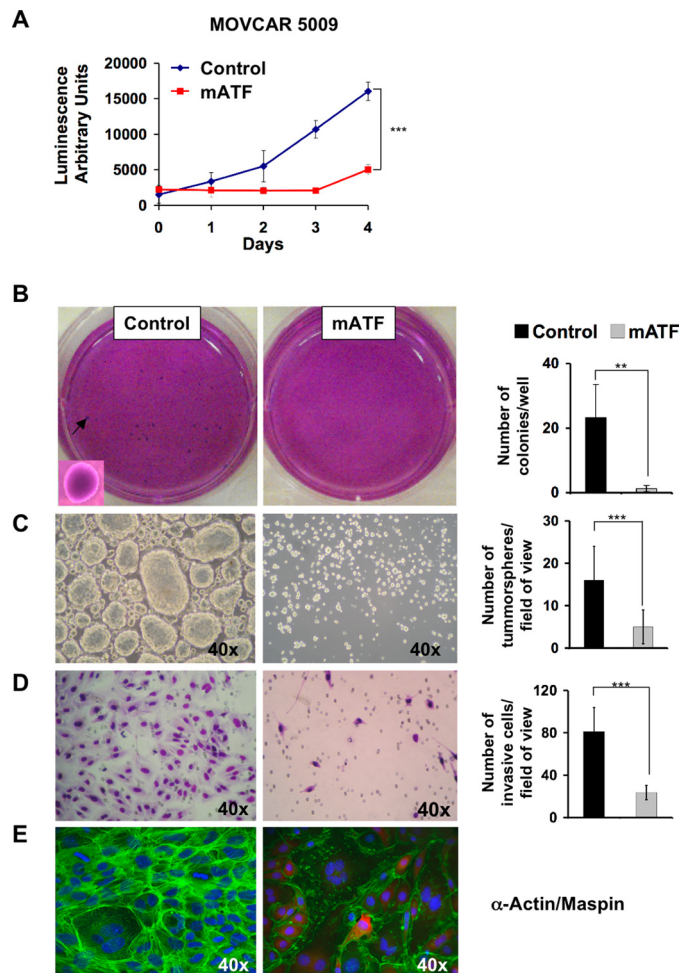

FIGURE 3. **mATF expression induces a decrease in tumor cell viability and invasion and promotes cytoskeleton disruption in the MOVCAR 5009 cell line.** *A*, retroviral delivery of mATF decreases cell viability over control-transduced cells as determined by Cell Titer Glo assay. Student's *t* test was applied to analyze the difference in tumor cell survival between the control and mATF cells, with $p < 0.001$. Three different transductions were performed, each one monitored in triplicate wells. *B*, mATF decreases anchorage-independent growth of MOVCAR 5009 cells. Soft agar colony formation assays were performed on control and mATF-transduced cells. The *arrow* in the picture (*left*) points to a colony amplified on the left corner. Colony quantification was performed 20 days after the seeding. Three independent experiments were carried out, and Student's *t* test was applied to analyze the data; $p = 0.0054$. *C*, mATF-transduced cells abolished tumor formation potential, as evaluated by tumorsphere assay formation. Cells were retrovirally transduced with either mATF or control and seeded in low-attachment culture plates with spheroid media (43). After 10 days, representative pictures of the experiment are shown outlining the abolishment of spheroid formation in mATF transduced cells. ($p = 0.0002$). *D*, mATF transduction in MOVCAR 5009 cells inhibits the invasion potential of the cells relative to control, as assessed by Matrigel-invasion assays (10). A representative picture of the fixed cells after 24 h of invasion is indicated. Three independent experiments were performed, and Student's *t* test was applied to analyze the data; $p = 0.0001$. *E*, immunofluorescence staining of actin (*green*) and Maspin (*red*) on mATF and control-transduced cells is shown. To detect actin, Alexa 488-phalloidin was applied, and anti-Maspin-Alexa 594 was used as the secondary antibody for Maspin detection. Hoechst 33258 was used to stain the nuclei (*blue*).

control. This result suggests that the mATF transduction was increasing the RNA-polymerase II binding in the *Maspin* promoter, resulting in an enhanced transcriptional activity, as confirmed by qRT-PCR and Western blot (Fig. 1, *B* and *C*).

The reactivation of *Maspin* by mATF in the MOVCAR 5009 cell line was further confirmed by immunofluorescence (Fig.

2*C*). In mATF-transduced cells, Maspin was found localized in the cytoplasm and in the nucleus of the tumor cells. When a *Maspin* cDNA-expressing retrovirus was used to exogenously express Maspin, only cytoplasmic Maspin was detected in the cells. The molecular basis of the differential Maspin localization observed between the mATF- and the cDNA-transduced cells is not known. A molecular hallmark of the ATFs is their ability
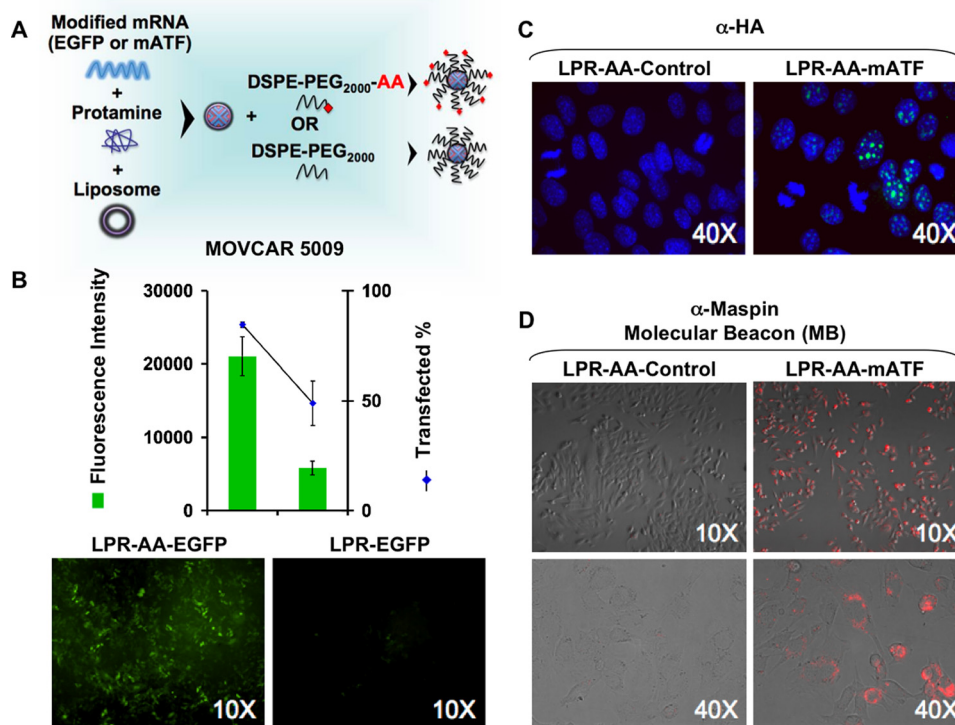
FIGURE 4. **Targeted LPR-AA nanoparticles encapsulating modified mATF mRNA results in functional production of the mATF and regulation of *Maspin* in the MOVCAR 5009 cell line.** *A*, shown is a schematic illustration of the generation of LPR-AA nanoparticles. The LPR nanoparticle core was prepared mixing modified mRNA (*e.g.* EGFP, mATF, or control, which is the mATF lacking the 5′ cap and is unable to translate) plus protamine and liposome. The LPR core was pegylated by adding either DSPE-PEG$_{2000}$-AA (targeted nanoparticle) or DSPE-PEG$_{2000}$ (non-targeted). *B*, MOVCAR 5009 cells were transfected with either LPR-AA-EGFP (targeted) or LPR-EGFP (non-targeted) nanoparticles, and the fluorescence intensity (quantification of the total fluorescence intensity of EGFP+ events) was measured by flow cytometry 24 h post-transfection by gating the percentage % of EGFP-positive cells. Cells treated with nanoparticle controls not carrying EGFP and untreated cells were used to generate the negative gates. A representative 10× picture of the transfected cells with LPR-AA-EGFP (targeted) or LPR-EGFP (non-targeted) nanoparticles is shown. *C*, shown is immunofluorescence detection of the mATF (*α-HA*, *green*) in MOVCAR 5009 cells. Cells were transfected with either LPR-AA-mATF or control (uncapped mATF mRNA). The cells were stained 24 h after transfection. *D*, real-time detection of *Maspin* in MOVCAR 5009 cells using an anti-*Maspin* molecular beacon (*MB*) is shown. Targeted nanoparticles containing either a functional mATF or an inactive control were also loaded with an anti-Maspin MB. Red fluorescence emission due to the hybridization of the *Maspin* transcript with the MB was detected 24 h post-transfection.

to activate the endogenous promoters (23), resulting in transcription of the physiologically relevant mRNA variants in the proper ratios, which represents a fundamental difference from the exogenous delivery of cDNAs (18).

mATF Expression Decreases Tumor Cell Viability and Inhibits Tumor Cell Invasion in MOVCAR 5009—To assess the effect of the mATF expression on the phenotype of MOVCAR 5009 cells, we first performed cell viability assays using a CellTiter Glo assay (Fig. 3*A*). The mATF-transduced cells and empty vector control were harvested 72 h post-transduction, and the cell viability was monitored every 24 h for a total of 4 days. We found that the ATF significantly decreased the tumor cell viability over time relative to control ($p < 0.001$). A significant decrease in cell viability was also observed when mATF was transduced in other MOVCAR cell lines carrying silenced *Maspin*, such as MOVCAR 5447 and 5612 (supplemental Fig. S2). Transduction of mATF also suppressed anchorage-independent growth of MOVCAR 5009 cells in soft agar colony formation assays (Fig. 3*B*). Furthermore, mATF completely suppressed the ability of MOVCAR 5009 cells to form tumorspheres in non-adherent plates, demonstrating that the engineered protein suppressed the tumorigenic properties of the cells *in vitro* (Fig. 3*C*). In addition to tumor suppression, *Maspin* re-expression in breast cancer cells has been associated

with decreased motility and invasion (10, 18, 49). Consistent with this second function of *Maspin*, we found that the mATF strongly suppressed the ability of MOVCAR 5009 cells to invade the Matrigel (Fig. 3*D*). Notably, the mATF-expressing cells underwent severe changes in cell shape, outlined by a disruption and loss of actin filaments (Fig. 3*E*).

LPR Nanoparticles Encapsulating a Chemically Modified mATF mRNA Are Efficiently Internalized into MOVCAR 5009 Cells in Vitro and in Tumor Allografts—We next investigated whether the mATF could be delivered in the tumor cells using a non-viral method by delivering chemically modified messenger RNA, eliminating the possibility of undesired genomic integration due to viral vector or plasmid DNA delivery. We generated LPR nanoparticles encapsulating the mATF mRNA. LPRs are liposome-based nanocarriers capable of delivering chemically modified RNAs to the targeted tumor site with high efficiency and specificity (Ref. 76; Fig. 4*A*). The chemical ligand anisamide (AA) was grafted at distal end PEG polymer on the surface of LPR particles to target the sigma receptors (SRs), which are overexpressed in a large spectrum of human tumors and cell lines (50). In our study we employed LPR-AA nanoparticle technology to deliver the mATF to the MOVCAR 5009 cell line. The expression of SR1 in MOVCAR 5009 cells was confirmed by Western blotting (supplemental Fig. S3). To evaluate the

transfection efficiency of the LPR-AA formulation, we encapsulated an mRNA encoding EGFP, and the expression level and percentage of EGFP$^+$ cells were evaluated by flow cytometry. As shown in Fig. 4*B*, MOVCAR 5009 cells were transfected with ~85% efficiency and, thus, with a yield comparable with retroviral or lentiviral vectors. In addition, the transfection efficiency was ligand-dependent. AA-LPR resulted in a 3-fold transgene expression reflected by fluorescence intensity and a 2-fold percent of transfected cells compared with non-targeted LPR. This implied that efficient gene delivery with high specificity was achieved as a result of enhanced receptor mediated cellular uptake. Next, we investigated whether the delivery of functional LPR-AA nanoparticles encapsulating the mATF mRNA resulted in efficient translation of the mATF and in nuclear localization of the designer protein. The expression of mATF was detected by immunohistochemistry using an anti-HA antibody to detect the C-terminal epitope tag of the protein. As shown in Fig. 4*C*, the functional mATF, but not an inactive control ATF mRNA without 5' cap structure, was detected in punctate structures in the nucleus of the cells, demonstrating effective translation. To investigate whether the mATF was transcriptionally competent in the cells, we co-transfected either the mATF mRNA or the uncapped ATF mRNA control, with a molecular beacon designed to specifically hybridize with *Maspin* mRNA. In the presence of untranslated control mRNA, no *Maspin* mRNA transcript was detected by the molecular beacon in the cells. However, when active mATF mRNA was included in the nanoparticle, an activation of endogenous *Maspin* mRNA was detected by the molecular beacon probe that allowed the real-time imaging of *Maspin* mRNA transcripts with a perinuclear localization (Fig. 4*D*). Overall, these studies demonstrated the delivery of our designer ZF protein into nanoparticles to target the ovarian cancer cells under study and effective mATF translation leading ultimately to *Maspin* re-expression.

At last, the ability of mATF-loaded nanoparticles to induce phenotypical changes in the cell line was evaluated *in vitro* (Fig. 5*A*). We found that LPR-AA-mATF nanoparticles significantly decreased survival of the MOVCAR 5009 cells by ~40% relative to control-loaded nanoparticles, as determined by a cell viability MTT assay (Fig. 5*A*). To assess the efficiency of LPR-AA nanoparticles to target MOVCAR 5009 cells *in vivo*, LPR-AA-mATF and control nanoparticles were delivered via intravenous injections into mice bearing MOVCAR 5009 subcutaneous allografts. Nanoparticle injections were performed via tail vein every 2 days with a total of 5 treatments. 24 days postinjection, a significant inhibition of tumor growth was detected on LPR-AA-mATF-injected animals relative to control ($p = 0.0220$) or vehicle-treated animals ($p = 0.0253$) (Fig. 5*B*). Tumors samples were processed by Western blot to demonstrate effective expression of the mATF in the tumors and concomitant *Maspin* regulation (Fig. 5*C*). In summary, these studies demonstrated that nanoparticle delivery of mATF mRNA led to a significant therapeutic effect inhibiting tumor cell growth of MOVCAR 5009 tumor allografts.

Genome-wide Changes in Gene Expression by mATF Delivery in MOVCAR 5009 Cells—To address the specificity of mATF in the MOVCAR 5009 cells, we performed gene expression
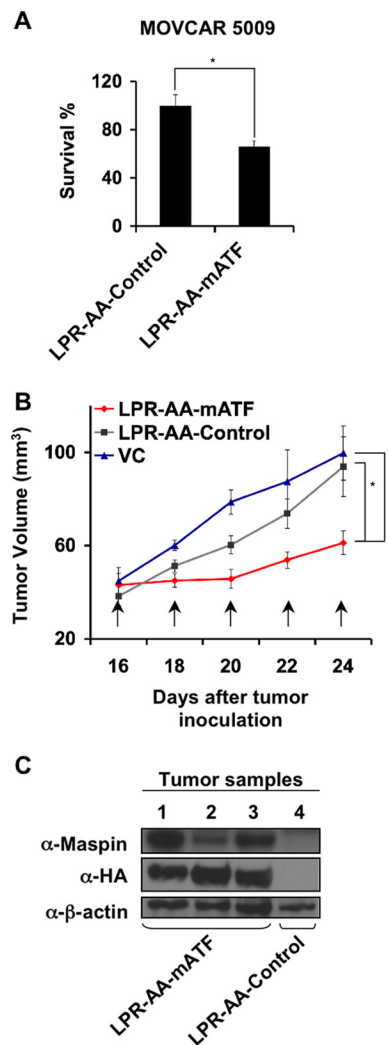

FIGURE 5. **Transfection of LPR-AA-mATF nanoparticles decreases the proliferation of MOVCAR 5009 cells *in vitro* and inhibits tumor growth *in vivo*.** *A*, delivery of LPR-AA-mATF nanoparticles decreases survival of MOVCAR 5009 cells relative to control-treated targeted nanoparticles. Cell survival was determined by MTT cell proliferation assay on cells transfected with either LPR-AA-mATF or control. Student's *t* test was applied to analyze the difference on survival between mATF and control-transfected cells; $p = 0.0002$. Data represent the averages and S.E. of three independent experiments, each one done in triplicate wells. *B*, LPR-AA-mATF nanoparticles inhibit the growth of MOVCAR 5009 cells in subcutaneous allografts in nude mice. MOVCAR 5009 cells were inoculated in nude mice to induce subcutaneous tumors, and nanoparticles were injected intravenously at the time points indicated in the graph (*arrows*). Student's *t* test was applied to analyze the difference between control ($n = 9$) and mATF treatment ($n = 9$; $p = 0.0220$) and between vehicle and mATF ($p = 0.0253$). *C*, mATF and Maspin expression were detected on the treated tumors by Western blot. An anti-HA antibody was used to detect the ATF by Western blot.

microarrays using Agilent mouse 4×180 K oligo microarrays. Cells were transduced in three independent biological replicates with either an empty retroviral vector (control) or with a mATF-expressing retrovirus. Significantly differentially expressed targets were analyzed using a two-class, unpaired SAM, with a false discovery rate <5%. Supplemental Tables S1 and S2 contain the list of genes significantly up-regulated (505 genes) and down-regulated (383 genes), respectively. A gene ontology (GO) analysis of the gene sets revealed gene pathways involved in nuclear signaling, signal transduction by small GTPases, cell motility, and adhesion (supplemental Table S3).

TABLE 1

Genes differentially regulated by mATF in the MOVCAR 5009 cell line

Name	Alias	-Fold change[a]	Function
Up-regulated genes			
Tetraspanin12	TM4SF12 TSPAN12	42.17	Member of the tetraspanin family of cell-surface proteins mediating signal transduction. (70)
Mammary serine protease inhibitor	Maspin SERPINB5	31.56	Tumor and metastasis suppressor gene. (27)
Calcium and integrin binding family member 2	CIB2 KIP2	30.79	A related family member, CIB1, regulates cell migration. (71)
Potassium large conductance calcium-activated channel, subfamily M, β member 4	KCNMB4 hβ4	29.07	Auxiliary β subunit on MaxiK channels, increases calcium sensitivity. (72)
Potassium channel tetramerisation domain containing 12	KCTD12 PFETIN	26.15	Positive prognostic biomarker in gastrointestinal tumors. (73)
Down-regulated genes			
Nidogen1	*NID1 Enactin*	0.0617	Suggested to play a role in cell interactions with the extracellular matrix. (74)
CCAAT/enhancer-binding protein δ	*CEBPD CELF*	0.1266	Up-regulated in breast (75) and lung (76) cancers.
Wingless-related MMTV integration site 10a	*WNT10A OODD*	0.1171	Activator on the Wnt-β-catenin-TCF signaling pathway (77).

[a] Relative to control (empty vector).

Notably, the gene expression microarray datasets revealed only 3 genes, including *Maspin*, with a relative mRNA up-regulation of 30-fold or higher over empty vector control (Table 1). These findings were validated by qRT-PCR, as indicated in Fig. 6*A*. The strongest mATF up-regulated target was *Maspin*, outlining the high degree of potency and specificity of the mATF in MOVCAR 5009 cells. The genes Tetraspanin12 (*Tspan12*), calcium and integrin binding family member 2 (*Cib2*), potassium channel tetramerization domain containing 12 (*Kctd12*), and potassium large conductance calcium-activated channel, subfamily M, β member 4 (*Kcnmb4*) were also found up-regulated in mATF-transduced samples relative to control-transduced or parental line ($p < 0.0001$). As shown in Table 1, the genes up-regulated by mATF are membrane-associated proteins involved in signal transduction, cell adhesion and migration, and tumor suppression. The down-regulated targets (≈ 0.13-fold relative to control) included potential oncogenes such as Wingless-related MMTV integration site 10a (*Wnt10a*) and CCAAT/enhancer binding protein δ (*Cebpd*) and regulators of cell adhesion, such as Nidogen1 (*Nid1*) (Fig. 6*B*). In summary, the analysis also revealed important novel targets co-regulated with *Maspin*, which could mediate the anti-metastatic and anti-tumorigenic phenotype of the ZF factor in EOC cell lines. Whether these targets represent indeed *bona fide* direct targets of the ATF or downstream genetic cascades of *Maspin* is presently not known and will require future molecular analyses, for example by zinc finger mapping in their promoter sites. However, these genome-wide data documented a high degree of potency and selectivity of mATF for its cognate *Maspin* target in MOVCAR 5009 cells.

Maspin and TSPAN12 Are Down-regulated in Short-term Cultures Derived from Human Ascites—We focused on the target TSPAN12, a member of the tetraspanin family of cell-surface proteins, some of which have been reported to mediate metastasis suppressive functions in several cancer models (51). We interrogated whether *TSPAN12* was co-regulated with *Maspin* in a panel of primary ovarian cancer tumors specimens and cell lines and whether the gene was silenced in ascites preparations from ovarian cancer patients. These samples were analyzed for *Maspin* and *TSPAN12* expression by qRT-PCR (Fig. 7*A*). Data were normalized to the SR06 sample, a normal total

ovary preparation. We found that *Maspin* was expressed in some ovarian primary tumors specimens and ovarian cell lines but was low or undetectable in most of the ascites samples. *TSPAN12* mRNA expression followed a similar pattern and was significantly lower in the vast majority of the ascites analyzed as compared with primary tumors and ovarian cancer cell lines. In one case examined, from which pair samples of tumor and ascites were available, the primary tumor (UC064) had significantly higher *Maspin* and *TSPAN12* mRNA expression than the ascites derived from the same patient (ASCUC064). As shown in Fig. 7*D* and supplemental Fig. S5, the expression of Maspin and TSPAN12 in primary EOC tumors was confirmed by immunofluorescence in epithelial ovarian cancer tissue specimens, Maspin having a predominantly cytoplasmic distribution, whereas TSPAN12 was localized on the plasma membrane. The down-regulation of Maspin and TSPAN12 in the short-term cultures from ascites fluids was also validated by Western blotting using the OVCAR-3 tumor cell line as reference (Fig. 7*B*).

The above results suggest that Maspin and TSPAN12 are down-regulated in metastatic cells, opening the possibility that TSPAN12 could be a downstream target of Maspin in ovarian cancer. Alternatively, TSPAN12 could be regulated as a result of mATF-dependent gene cascades, for example, by direct binding of the ATF or by indirect regulation of downstream targets. To address whether the activation of *TSPAN12* in mATF-transduced cells was dependent on *Maspin*, we challenged MOVCAR 5009 cells transduced with mATF with either a *Maspin*-specific siRNA or a control siRNA. Changes in *TSPAN12* were assessed in the transfected cells by qRT-PCR. As shown in Fig. 7*C*, the *Maspin* knockdown resulted in a significant down-regulation of *TSPAN12* in the MOVCAR 5009 cells, suggesting that *Maspin* could be controlling *TSPAN12* activation in these cells. In addition, we were unable to find putative binding sites of the mATF in the *TSPAN12* promoter, suggesting that *TSPAN12* is not a direct target of the ATF. Moreover, more analyses need to be done, for example, using genome-wide ZF mapping to validate the exact number and genomic location of all mATF-binding sites in the cancer cell genome. In summary, the gene expression analyses demonstrated that the ZF technology could be used for cancer inves-
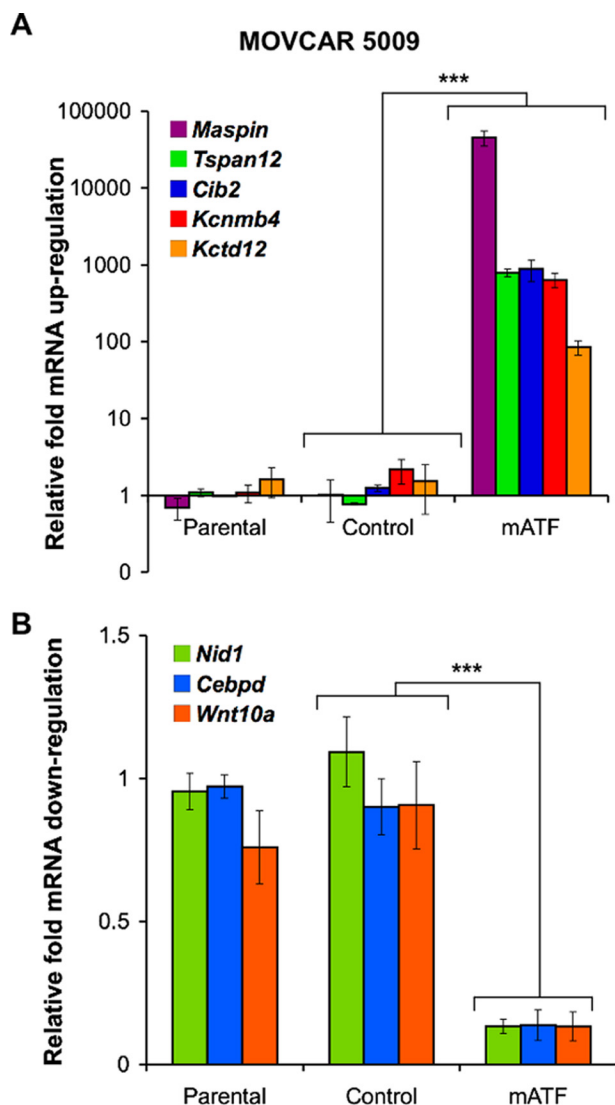
A

B

FIGURE 6. **mRNA quantification of targets up- and down-regulated by mATF in MOVCAR 5009 cells.** Changes in mRNA expression of genes previously identified by gene expression microarrays (supplemental Table S1 and Table S2) were validated by qRT-PCR. *A*, genes differentially up-regulated by transduction of mATF in MOVCAR 5009 cells are shown. *B*, genes down-regulated by mATF are shown. Data were normalized to the parental MOVCAR 5009 cell line and represent the mean and S.D. of at least three independent experiments. Differences in gene expression were calculated with a student *t* test; ***, $p \leq 0.0001$.

tigators to identify novel targets potentially involved in migration and metastatic progression for future diagnosis and treatment of aggressive metastatic disease.

DISCUSSION

Mammary serine protease inhibitor (*Maspin*) has emerged as an important clinical target possessing tumor and metastasis suppressive functions. Although the function of *Maspin* has been well examined in breast (52), lung (53), and prostate (54) models, its function as a tumor and metastasis suppressor in ovarian cancer has not been well investigated. In this paper we took advantage of ZF technology to interrogate the role of *Maspin* in metastatic ovarian cancer. We have described an mATF able to up-regulate endogenous *Maspin* in metastatic murine ovarian cancer cell lines derived from a Tg*MISRII-TAg* GEMM

of serous ovarian cancer (9). The mATF had an exceptionally strong transcriptional activation in multiple murine cancer cell models derived from GEMMs, with levels of expression that were comparable with ectopic cDNA overexpression. The higher transcriptional potency of the mATF relative to the previously reported human-specific ATF (ATF-126) could be related to the configuration of the chromatin and the promoter context of the mouse promoter. Moreover, MOVCAR 5009 cells derived from ascitic fluids from the C57BL/6 Tg*MISRII-TAg* GEMM exhibited an epigenetically silenced *Maspin*, which could be partially re-activated by DNA methyltransferase (DNMT) and histone deacetylase inhibitors. In this background the mATF was able to bind its target site in the cell and reactivated *Maspin* mRNA expression by more than 70,000-fold relative to control-transduced and parental cells. The much higher potency of the ATF in activating *Maspin* relative to chromatin remodelers could be explained by the fact that the ZFs confer locus selectivity. In contrast, epigenetic inhibitors, such as DNA methyltransferase (DNMT) and histone deacetylase inhibitors, are believed to target a large spectrum of tumor suppressors. In addition, the *Maspin*-specific ZFs are linked to the VP64 transactivator domain, which enhances transcription by recruitment of several components of the transcription machinery (55). Consistently, our ChIP analysis demonstrated an enrichment of RNA-polymerase II binding in the *Maspin* promoter upon mATF overexpression. Interestingly, the transduction of mATF elevated both cytoplasmic and nuclear forms of Maspin, whereas the exogenous cDNA overexpression up-regulated only cytosolic Maspin. Recent publications outline the importance of nuclear Maspin as being a favorable prognosis factor in breast (56), lung (57), and ovarian carcinomas (33). This result emphasizes the significance of the endogenous mechanisms of regulation of targeted promoters, which results in activation of the physiologically relevant isoform of the targeted gene. The phenotypic outcomes of *Maspin* reactivation in metastatic MOVCAR 5009 cells recapitulated the effect of the human ATF-126 in breast cancer models (10, 18). Retroviral delivery of mATF resulted in decreased cell viability, tumorigenicity, and strongly suppressed cell invasion. mATF induced profound remodeling in the actin cytoskeleton, which could have a negative impact in cell adhesion, migration, and mitosis. mATF-transduction induced the formation of multiple focal adhesions, indicating the cells were less prone to migration.

Our data are consistent with previous studies showing that treatment with a recombinant Maspin protein, rMaspin, resulted in increased adhesion and inhibition of cell invasion of the breast carcinoma MDA-MB-435 cell line (58). rMaspin led to changes in the cytoskeleton structure and increased the formation of focal adhesions in metastatic breast cancer cells (59). Our results with our designer protein confirm the role of *Maspin* as metastasis suppressor in metastatic ovarian cancer by modulating cell surface signaling pathways resulting in cytoskeleton remodeling.

To evaluate the specificity of the mATF in MOVCAR 5009 cells and to identify genes mediating the anti-tumor/metastatic phenotype of the protein, we performed genome-wide gene expression microarrays. These analyses revealed that only two
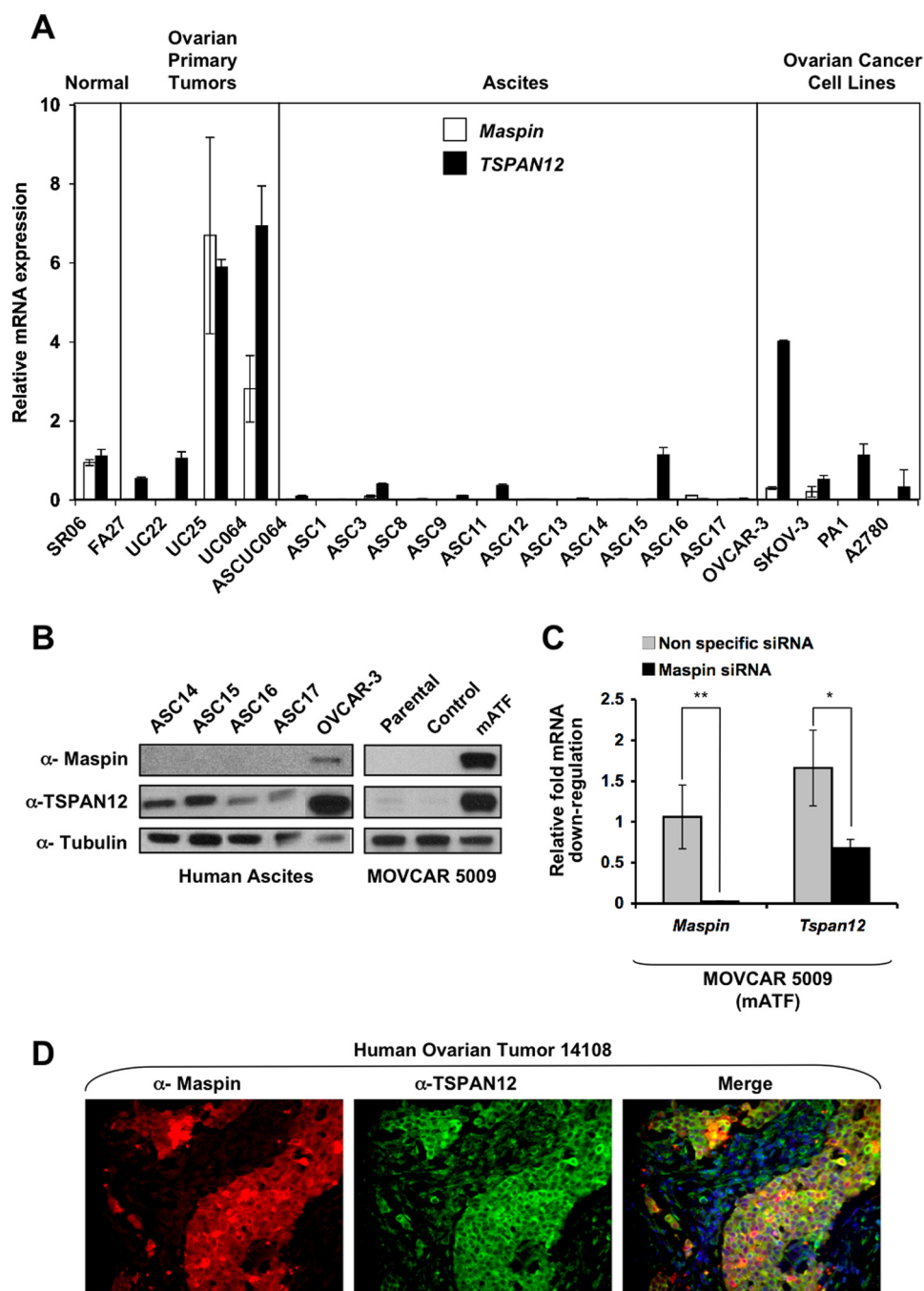
FIGURE 7. **Down-regulation of *Maspin* and *TSPAN12* in short term human ascites preparations from ovarian carcinoma patients.** *A*, expression of *Maspin* and *TSPAN12* in a panel of human ovarian primary tumors, ascites, and established cancer cell lines, as assessed by qRT-PCR is shown. Data were normalized to SR06, a preparation of normal ovary. UC064 and ASCUC064 represent tumor sample and ascites preparation, respectively, from the same patient. Tumor specimens, ascites preparations, and ovarian cell lines were homogenized and resuspended in Trizol for mRNA extraction and analyzed by quantitative qRT-PCR. *B*, shown is an immunoblot of Maspin and TSPAN12 on protein extracts from human ascites, the human cell line OVCAR-3, and parental, control, and mATF-transduced MOVCAR 5009 cells. *C*, down-regulation of *Maspin* and *Tspan12* after Maspin siRNA knockdown in the mATF-transduced MOVCAR 5009 cell line as assessed by qRT-PCR is shown. Data were normalized to the cell line transfected with a control (anti-luciferase) siRNA (*, $p \leq 0.05$; **, $p \leq 0.01$; ***, $p \leq 0.001$). *D*, shown is expression of Maspin and TSPAN12 by immunofluorescence in representative sections of epithelial ovarian cancer specimens (see also supplemental Fig. S5).

targets were up-regulated together with *Maspin*, with a -fold overexpression higher than 30 relative to control-transduced cells. The subsequent qRT-PCR validation of these targets demonstrated that *Maspin* was the most regulated target of the ATF, outlining the high potency and specificity of the engineered factor.

TSPAN12 belongs to the tetraspanin family of signal transduction proteins, many of which act as tumor suppressors and regulators of metastasis (51). Tetraspanins are transmembrane proteins that physically associate with integrins to transduce signals inside the cell (60). CD9 is a tetraspanin involved in regulation of cell adhesion and motility (61). Down-regulation

of tetraspanin CD9 has been associated with metastatic behavior and poor prognosis in lung (62), breast (63), and ovarian cancers (64). CD9 down-regulates the expression of several Wnt-associated proteins in lung adenocarcinoma and fibrosarcoma cell lines (65). Interestingly, mATF delivery in MOVCAR 5009 cells led to an up-regulation of (TSPAN12) and a down-regulation of Wnt10a suggesting that modulation of Wnt signaling could be of therapeutic value for treatment of metastatic ovarian cancer. Our results identified a novel target, *TSPAN12*, that was found down-regulated together with *Maspin* in human metastatic ovarian cancer cells derived from ascites. In summary, these results demonstrate that ZF could be used to potentially discover novel molecular targets and regulators of metastasis in ovarian cancer.

Delivery of ZF proteins has been an unbearable problem for the transition of these agents into the clinic. In addition to effective delivery in pre-existing tumors, another fundamental problem is the specificity to the tumor tissue. To deliver the mATF in MOVCAR 5009 tumor allografts, we developed LPR-AA nanoparticles. The anisamide (AA) ligand coated at the surface of the particles provides specificity for the sigma receptor (SR1) (44), which is expressed at high levels in a vast spectrum of cancer cell lines (50), including the MOVCAR 5009 cells. These nanoparticles were designed with a condensed core comprising protamine and a chemically modified mATF mRNA. The delivery of modified mRNA circumvents limitations associated with traditional plasmid DNA, such as nuclear delivery of DNA through the nuclear envelope and host immunoresponse (76). *In vitro* synthesis of chemically modified RNA using ribonucleotide analogues has been shown to suppress the innate immune response by stimulating toll-like receptor and concomitantly extend the half-life of the mRNA molecule (66). Previous work has demonstrated that chemically modified mRNA can be used for delivery of reprogramming transcription factors for inducible pluripotent stem cells *in vitro* (66). Indeed, we have found that our LPR-AA nanoparticles transfected MOVCAR 5009 cells with efficiencies similar to retroviral delivery (~60%). In addition, the same LPR formulation was able to transfect some breast cancer cell lines with efficiencies close to 100% (data not shown) outlining the potential of the technology to effectively deliver ZF proteins in tumor models. The LPR nanoparticles were formulated such that high density of hydrophilic PEG was coated on the surface of the nanoparticles. The PEG coating stabilized LPR in the presence of serum proteins and reduced nonspecific uptake by reticuloendothelial system, extending the half-life in the blood circulation after systemic administration. This led to the enhanced tumor accumulation due to the enhanced permeability and retention. Notably, we demonstrated that the LPR-mATF-AA nanoparticles resulted in translation of ZF proteins in the tumor cells and in transactivation of the endogenous Maspin. When delivered intravenously in a MOVCAR 5009 allograft model, the LPR-mATF-AA nanoparticles significantly inhibited tumor growth, which was accompanied by *Maspin* reactivation in the tumors. These results are very encouraging and provide the first non-viral delivery of ZF proteins *in vivo* for its potential use in clinical trials to treat metastatic disease. Although our results demonstrate proof-of-concept using nude mice, the next step will

require the intravenous injection of LPRs in a syngeneic or even in the GEMM C57BL/6 Tg*MISRII-TAg* of ovarian cancer, which develops ovarian cancer in a similar progression as in humans (9). In addition, future research will involve the intraperitoneal injection of LPRs in mice carrying abdominal metastases to assess the efficiency of the mATF to abolish pre-established metastases. Given the explosion of publications using both ZF and transcription activator-like effectors (TALEs) technologies in the past decade (particularly in the domain of gene therapy (67)), our results provide a novel non-viral delivery system of mRNA to be used for a broad spectrum of investigators working in the area of designer ZF factors.

REFERENCES

1. Jemal, A., Bray, F., Center, M. M., Ferlay, J., Ward, E., and Forman, D. (2011) Global cancer statistics. *CA Cancer J. Clin.* **61,** 69–90
2. Rosen, D. G., Yang, G., Liu, G., Mercado-Uribe, I., Chang, B., Xiao, X. S., Zheng, J., Xue, F. X., and Liu, J. (2009) Ovarian cancer. Pathology, Biology, and Disease models. *Front Biosci.* **14,** 2089–2102
3. Havrilesky, L., Darcy, M., Hamdan, H., Priore, R. L., Leon, J., Bell, J., and Berchuck, A. (2003) Prognostic significance of p53 mutation and p53 overexpression in advanced epithelial ovarian cancer. A gynecologic oncology group study. *J. Clin. Oncol.* **21,** 3814–3825
4. Risch, H. A., McLaughlin, J. R., Cole, D. E., Rosen, B., Bradley, L., Kwan, E., Jack, E., Vesprini, D. J., Kuperstein, G., Abrahamson, J. L., Fan, I., Wong, B., and Narod, S. A. (2001) Prevalence and penetrance of germline BRCA1 and BRCA2 mutations in a population series of 649 women with ovarian cancer. *Am. J. Hum. Genet.* **68,** 700–710
5. Liu, J., and Matulonis, U. A. (2010) New advances in ovarian cancer. *Oncology* **24,** 721–728
6. Gardner, G. J., and Jewell, E. L. (2011) Current and future directions of clinical trials for ovarian cancer. *Cancer Control* **18,** 44–51
7. Berkenblit, A., and Cannistra, S. A. (2005) Advances in the management of epithelial ovarian cancer. *J. Reprod. Med.* **50,** 426–438
8. Connolly, D. C. (2009) Animal models of ovarian cancer. *Cancer Treat. Res.* **149,** 353–391
9. Quinn, B. A., Xiao, F., Bickel, L., Martin, L., Hua, X., Klein-Szanto, A., and Connolly, D. C. (2010) Development of a syngeneic mouse model of epithelial ovarian cancer. *J. Ovarian Res.* **3,** 24
10. Beltran, A., Parikh, S., Liu, Y., Cuevas, B. D., Johnson, G. L., Futscher, B. W., and Blancafort, P. (2007) Reactivation of a dormant tumor suppressor gene maspin by designed transcription factors. *Oncogene* **26,** 2791–2798
11. Pavletich, N. P., and Pabo, C. O. (1991) Zinc finger-DNA recognition. Crystal structure of a Zif268-DNA complex at 2.1 Å. *Science* **252,** 809–817
12. Liu, Q., Segal, D. J., Ghiara, J. B., and Barbas, C. F., 3rd. (1997) Design of polydactyl zinc-finger proteins for unique addressing within complex genomes. *Proc. Natl. Acad. Sci. U.S.A.* **94,** 5525–5530
13. Blancafort, P., and Beltran, A. S. (2008) Rational design, selection. and specificity of artificial transcription factors (ATFs). The influence of chromatin in target gene regulation. *Comb. Chem. High Throughput Screen* **11,** 146–158
14. Beltran, A., Liu, Y., Parikh, S., Temple, B., and Blancafort, P. (2006) Interrogating genomes with combinatorial artificial transcription factor libraries. Asking zinc finger questions. *Assay Drug Dev. Technol.* **4,** 317–331
15. Beltran, A. S., and Blancafort, P. (2011) Reactivation of MASPIN in non-small cell lung carcinoma (NSCLC) cells by artificial transcription factors (ATFs). *Epigenetics* **6,** 224–235

16. Beltran, A. S., and Blancafort, P. (2010) Remodeling genomes with artificial transcription factors (ATFs). *Methods Mol. Biol.* **649,** 163–182

17. Beltran, A. S., Sun, X., Lizardi, P. M., and Blancafort, P. (2008) Reprogramming epigenetic silencing. Artificial transcription factors synergize with chromatin remodeling drugs to reactivate the tumor suppressor mammary serine protease inhibitor. *Mol. Cancer Ther.* **7,** 1080–1090

18. Beltran, A. S., Russo, A., Lara, H., Fan, C., Lizardi, P. M., and Blancafort, P. (2011) Suppression of breast tumor growth and metastasis by an engineered transcription factor. *PLoS One* **6,** e24595

19. Zhang, L., Spratt, S. K., Liu, Q., Johnstone, B., Qi, H., Raschke, E. E., Jamieson, A. C., Rebar, E. J., Wolffe, A. P., and Case, C. C. (2000) Synthetic zinc finger transcription factor action at an endogenous chromosomal site. Activation of the human erythropoietin gene. *J. Biol. Chem.* **275,** 33850–33860

20. Liu, P. Q., Rebar, E. J., Zhang, L., Liu, Q., Jamieson, A. C., Liang, Y., Qi, H., Li, P. X., Chen, B., Mendel, M. C., Zhong, X., Lee, Y. L., Eisenberg, S. P., Spratt, S. K., Case, C. C., and Wolffe, A. P. (2001) Regulation of an endogenous locus using a panel of designed zinc finger proteins targeted to accessible chromatin regions. Activation of vascular endothelial growth factor A. *J. Biol. Chem.* **276,** 11323–11334

21. Beerli, R. R., Dreier, B., and Barbas, C. F., 3rd. (2000) Positive and negative regulation of endogenous genes by designed transcription factors. *Proc. Natl. Acad. Sci. U.S.A.* **97,** 1495–1500

22. Dreier, B., Beerli, R. R., Segal, D. J., Flippin, J. D., and Barbas, C. F., 3rd. (2001) Development of zinc finger domains for recognition of the 5'-ANN-3' family of DNA sequences and their use in the construction of artificial transcription factors. *J. Biol. Chem.* **276,** 29466–29478

23. Beerli, R. R., and Barbas, C. F., 3rd. (2002) Engineering polydactyl zinc finger transcription factors. *Nat. Biotechnol.* **20,** 135–141

24. Beerli, R. R., Segal, D. J., Dreier, B., and Barbas, C. F., 3rd. (1998) Toward controlling gene expression at will. Specific regulation of the erbB-2/HER-2 promoter by using polydactyl zinc finger proteins constructed from modular building blocks. *Proc. Natl. Acad. Sci. U.S.A.* **95,** 14628–14633

25. Blancafort, P., Chen, E. I., Gonzalez, B., Bergquist, S., Zijlstra, A., Guthy, D., Brachat, A., Brakenhoff, R. H., Quigley, J. P., Erdmann, D., and Barbas, C. F., 3rd. (2005) Genetic reprogramming of tumor cells by zinc finger transcription factors. *Proc. Natl. Acad. Sci. U.S.A.* **102,** 11716–11721

26. Durai, S., Mani, M., Kandavelou, K., Wu, J., Porteus, M. H., and Chandrasegaran, S. (2005) Zinc finger nucleases. Custom-designed molecular scissors for genome engineering of plant and mammalian cells. *Nucleic Acids Res.* **33,** 5978–5990

27. Zou, Z., Anisowicz, A., Hendrix, M. J., Thor, A., Neveu, M., Sheng, S., Rafidi, K., Seftor, E., and Sager, R. (1994) Maspin, a serpin with tumor-suppressing activity in human mammary epithelial cells. *Science* **263,** 526–529

28. Futscher, B. W., Oshiro, M. M., Wozniak, R. J., Holtan, N., Hanigan, C. L., Duan, H., and Domann, F. E. (2002) Role for DNA methylation in the control of cell type specific maspin expression. *Nat. Genet.* **31,** 175–179

29. Goulet, B., Kennette, W., Ablack, A., Postenka, C. O., Hague, M. N., Mymryk, J. S., Tuck, A. B., Giguère, V., Chambers, A. F., and Lewis, J. D. (2011) Nuclear localization of maspin is essential for its inhibition of tumor growth and metastasis. *Lab. Invest.* **91,** 1181–1187

30. Rose, S. L., Fitzgerald, M. P., White, N. O., Hitchler, M. J., Futscher, B. W., De Geest, K., and Domann, F. E. (2006) Epigenetic regulation of maspin expression in human ovarian carcinoma cells. *Gynecol. Oncol.* **102,** 319–324

31. Beltran, A. S., and Blancafort, P. (2011) Reactivation of MASPIN in non-small cell lung carcinoma (NSCLC) cells by artificial transcription factors (ATFs). *Epigenetics* **6,** 224–235

32. Sood, A. K., Fletcher, M. S., Gruman, L. M., Coffin, J. E., Jabbari, S., Khalkhali-Ellis, Z., Arbour, N., Seftor, E. A., and Hendrix, M. J. (2002) The paradoxical expression of maspin in ovarian carcinoma. *Clin. Cancer Res.* **8,** 2924–2932

33. Solomon, L. A., Munkarah, A. R., Schimp, V. L., Arabi, M. H., Morris, R. T., Nassar, H., and Ali-Fehmi, R. (2006) Maspin expression and localization impact on angiogenesis and prognosis in ovarian cancer. *Gynecol. Oncol.* **101,** 385–389

34. Sopel, M., Surowiak, P., and Berdowska, I. (2010) Nuclear maspin expression as a good prognostic factor in human epithelial ovarian carcinoma. *Folia Morphol. (Warsz)* **69,** 204–212

35. Herschkowitz, J. I., Zhao, W., Zhang, M., Usary, J., Murrow, G., Edwards, D., Knezevic, J., Greene, S. B., Darr, D., Troester, M. A., Hilsenbeck, S. G., Medina, D., Perou, C. M., and Rosen, J. M. (2011) Comparative oncogenomics identifies breast tumors enriched in functional tumor-initiating cells. *Proc. Natl. Acad. Sci. U.S.A.* **109,** 2778–2783

36. Holzer, R. G., MacDougall, C., Cortright, G., Atwood, K., Green, J. E., and Jorcyk, C. L. (2003) Development and characterization of a progressive series of mammary adenocarcinoma cell lines derived from the C3(1)/SV40 Large T-antigen transgenic mouse model. *Breast Cancer Res. Treat* **77,** 65–76

37. Svirshchevskaya, E. V., Mariotti, J., Wright, M. H., Viskova, N. Y., Telford, W., Fowler, D. H., and Varticovski, L. (2008) Rapamycin delays growth of Wnt-1 tumors in spite of suppression of host immunity. *BMC Cancer* **8,** 176

38. Wright, M. H., Calcagno, A. M., Salcido, C. D., Carlson, M. D., Ambudkar, S. V., and Varticovski, L. (2008) Brca1 breast tumors contain distinct CD44+/CD24- and CD133+ cells with cancer stem cell characteristics. *Breast Cancer Res.* **10,** R10

39. Wright, M. H., Robles, A. I., Herschkowitz, J. I., Hollingshead, M. G., Anver, M. R., Perou, C. M., and Varticovski, L. (2008) Molecular analysis reveals heterogeneity of mouse mammary tumors conditionally mutant for Brca1. *Mol. Cancer* **7,** 29

40. MacLachlan, T. K., and El-Deiry, W. S. (2003) Identification of DNA binding of tumor suppressor genes by chromatin immunoprecipitation. *Methods Mol. Biol.* **223,** 129–133

41. Rice, J. C., and Futscher, B. W. (2000) Transcriptional repression of BRCA1 by aberrant cytosine methylation, histone hypoacetylation, and chromatin condensation of the BRCA1 promoter. *Nucleic Acids Res.* **28,** 3233–3239

42. Lu, Y. C., Song, J., Cho, H. Y., Fan, G., Yokoyama, K. K., and Chiu, R. (2006) Cyclophilin a protects Peg3 from hypermethylation and inactive histone modification. *J. Biol. Chem.* **281,** 39081–39087

43. Beltran, A. S., Rivenbark, A. G., Richardson, B. T., Yuan, X., Quian, H., Hunt, J. P., Zimmerman, E., Graves, L. M., and Blancafort, P. (2011) Generation of tumor-initiating cells by exogenous delivery of OCT4 transcription factor. *Breast Cancer Res.* **13,** R94

44. Banerjee, R., Tyagi, P., Li, S., and Huang, L. (2004) Anisamide-targeted stealth liposomes. a potent carrier for targeting doxorubicin to human prostate cancer cells. *Int. J. Cancer* **112,** 693–700

45. Li, Y. L., Ye, F., Hu, Y., Lu, W. G., and Xie, X. (2009) Identification of suitable reference genes for gene expression studies of human serous ovarian cancer by real-time polymerase chain reaction. *Anal. Biochem.* **394,** 110–116

46. Fu, J., Bian, L., Zhao, L., Dong, Z., Gao, X., Luan, H., Sun, Y., and Song, H. (2010) Identification of genes for normalization of quantitative real-time PCR data in ovarian tissues. *Acta Biochim. Biophys. Sin.* **42,** 568–574

47. Herschkowitz, J. I., Simin, K., Weigman, V. J., Mikaelian, I., Usary, J., Hu, Z., Rasmussen, K. E., Jones, L. P., Assefnia, S., Chandrasekharan, S., Backlund, M. G., Yin, Y., Khramtsov, A. I., Bastein, R., Quackenbush, J., Glazer, R. I., Brown, P. H., Green, J. E., Kopelovich, L., Furth, P. A., Palazzo, J. P., Olopade, O. I., Bernard, P. S., Churchill, G. A., Van Dyke, T., and Perou, C. M. (2007) Identification of conserved gene expression features between murine mammary carcinoma models and human breast tumors. *Genome Biol.* **8,** R76

48. Hosack, D. A., Dennis, G., Jr., Sherman, B. T., Lane, H. C., and Lempicki, R. A. (2003) Identifying biological themes within lists of genes with EASE. *Genome Biol.* **4,** R70

49. Sheng, S., Carey, J., Seftor, E. A., Dias, L., Hendrix, M. J., and Sager, R. (1996) Maspin acts at the cell membrane to inhibit invasion and motility of mammary and prostatic cancer cells. *Proc. Natl. Acad. Sci. U.S.A.* **93,** 11669–11674

50. Aydar, E., Onganer, P., Perrett, R., Djamgoz, M. B., and Palmer, C. P. (2006) The expression and functional characterization of δ1 receptors in breast cancer cell lines. *Cancer Lett.* **242,** 245–257

51. Richardson, M. M., Jennings, L. K., and Zhang, X. A. (2011) Tetraspanins

and tumor progression. *Clin. Exp. Metastasis* **28,** 261–270

52. Endsley, M. P., and Zhang, M. (2011) Investigating maspin in breast cancer progression using mouse models. *Methods Enzymol.* **499,** 149–165

53. Lonardo, F., Li, X., Kaplun, A., Soubani, A., Sethi, S., Gadgeel, S., and Sheng, S. (2010) The natural tumor suppressor protein maspin and potential application in non-small cell lung cancer. *Curr. Pharm. Des.* **16,** 1877–1881

54. Zou, Z., Zhang, W., Young, D., Gleave, M. G., Rennie, P., Connell, T., Connelly, R., Moul, J., Srivastava, S., and Sesterhenn, I. (2002) *Clin. Cancer Res.* **8,** 1172–1177

55. Herrera, F. J., and Triezenberg, S. J. (2004) VP16-dependent association of chromatin-modifying coactivators and underrepresentation of histones at immediate-early gene promoters during herpes simplex virus infection. *J. Virol.* **78,** 9689–9696

56. Mohsin, S. K., Zhang, M., Clark, G. M., and Craig Allred, D. (2003) Maspin expression in invasive breast cancer. Association with other prognostic factors. *J. Pathol.* **199,** 432–435

57. Lonardo, F., Li, X., Siddiq, F., Singh, R., Al-Abbadi, M., Pass, H. I., and Sheng, S. (2006) Maspin nuclear localization is linked to favorable morphological features in pulmonary adenocarcinoma. *Lung Cancer* **51,** 31–39

58. Seftor, R. E., Seftor, E. A., Sheng, S., Pemberton, P. A., Sager, R., and Hendrix, M. J. (1998) maspin suppresses the invasive phenotype of human breast carcinoma. *Cancer Res.* **58,** 5681–5685

59. Odero-Marah, V. A., Khalkhali-Ellis, Z., Chunthapong, J., Amir, S., Seftor, R. E., Seftor, E. A., and Hendrix, M. J. (2003) Maspin regulates different signaling pathways for motility and adhesion in aggressive breast cancer cells. *Cancer Biol. Ther.* **2,** 398–403

60. Hemler, M. E. (2005) Tetraspanin functions and associated microdomains. *Nat. Rev. Mol. Cell Biol.* **6,** 801–811

61. Ikeyama, S., Koyama, M., Yamaoko, M., Sasada, R., and Miyake, M. (1993) Suppression of cell motility and metastasis by transfection with human motility-related protein (MRP-1/CD9) DNA. *J. Exp. Med.* **177,** 1231–1237

62. Higashiyama, M., Doi, O., Kodama, K., Yokouchi, H., Adachi, M., Huang, C. L., Taki, T., Kasugai, T., Ishiguro, S., Nakamori, S., and Miyake, M. (1997) Immunohistochemically detected expression of motility-related protein-1 (MRP-1/CD9) in lung adenocarcinoma and its relation to prognosis. *Int. J. Cancer* **74,** 205–211

63. Huang, C. I., Kohno, N., Ogawa, E., Adachi, M., Taki, T., and Miyake, M. (1998) Correlation of reduction in MRP-1/CD9 and KAI1/CD82 expression with recurrences in breast cancer patients. *Am. J. Pathol.* **153,** 973–983

64. Furuya, M., Kato, H., Nishimura, N., Ishiwata, I., Ikeda, H., Ito, R., Yoshiki, T., and Ishikura, H. (2005) Down-regulation of CD9 in human ovarian carcinoma cell might contribute to peritoneal dissemination. Morphologic alteration and reduced expression of $\beta1$ integrin subsets. *Cancer Res.* **65,** 2617–2625

65. Huang, C. L., Liu, D., Masuya, D., Kameyama, K., Nakashima, T., Yokomise, H., Ueno, M., and Miyake, M. (2004) MRP-1/CD9 gene transduction down-regulates Wnt signal pathways. *Oncogene* **23,** 7475–7483

66. Warren, L., Manos, P. D., Ahfeldt, T., Loh, Y. H., Li, H., Lau, F., Ebina, W., Mandal, P. K., Smith, Z. D., Meissner, A., Daley, G. Q., Brack, A. S., Collins, J. J., Cowan, C., Schlaeger, T. M., and Rossi, D. J. (2010) Highly efficient reprogramming to pluripotency and directed differentiation of human cells with synthetic modified mRNA. *Cell Stem Cell* **7,** 618–630

67. Mussolino, C., and Cathomen, T. (2012) TALE nucleases. Tailored genome engineering made easy. *Curr. Opin. Biotechnol.*, in press

68. Wu, H., Yang, W. P., and Barbas, C. F., 3rd. (1995) Building zinc fingers by selection. Toward a therapeutic application. *Proc. Natl. Acad. Sci. U.S.A.* **92,** 344–348

69. Blancafort, P., Magnenat, L., and Barbas, C. F., 3rd. (2003) Scanning the human genome with combinatorial transcription factor libraries. *Nat. Biotechnol.* **21,** 269–274

70. Wang, H. X., Li, Q., Sharma, C., Knoblich, K., and Hemler, M. E. (2011) Tetraspanin protein contributions to cancer. *Biochem. Soc. Trans.* **39,** 547–552

71. Leisner, T. M., Liu, M., Jaffer, Z. M., Chernoff, J., and Parise, L. V. (2005) Essential role of CIB1 in regulating PAK1 activation and cell migration. *J. Cell Biol.* **170,** 465–476

72. Brenner, R., Jegla, T. J., Wickenden, A., Liu, Y., and Aldrich, R. W. (2000) Cloning and functional characterization of novel large conductance calcium-activated potassium channel β subunits, hKCNMB3 and hKCNMB4. *J. Biol. Chem.* **275,** 6453–6461

73. Suehara, Y., Kondo, T., Seki, K., Shibata, T., Fujii, K., Gotoh, M., Hasegawa, T., Shimada, Y., Sasako, M., Shimoda, T., Kurosawa, H., Beppu, Y., Kawai, A., and Hirohashi, S. (2008) Pfetin as a prognostic biomarker of gastrointestinal stromal tumors revealed by proteomics. *Clin. Cancer Res.* **14,** 1707–1717

74. Miosge, N., Holzhausen, S., Zelent, C., Sprysch, P., and Herken, R. (2001) Nidogen-1 and nidogen-2 are found in basement membranes during human embryonic development. *Histochem. J.* **33,** 523–530

75. Milde-Langosch, K., Löning, T., and Bamberger, A. M. (2003) Expression of the CCAAT/enhancer-binding proteins C/EBPα, C/EBPβ, and C/EBPδ in breast cancer. Correlations with clinicopathologic parameters and cell-cycle regulatory proteins. *Breast Cancer Res. Treat.* **79,** 175–185

76. Min, Y., Ghose, S., Boelte, K., Li, J., Yang, L., and Lin, P. C. (2011) C/EBP-δ regulates VEGF-C autocrine signaling in lymphangiogenesis and metastasis of lung cancer through HIF-1α. *Oncogene* **30,** 4901–4909

77. Yasuniwa, Y., Izumi, H., Wang, K. Y., Shimajiri, S., Sasaguri, Y., Kawai, K., Kasai, H., Shimada, T., Miyake, K., Kashiwagi, E., Hirano, G., Kidani, A., Akiyama, M., Han, B., Wu, Y., Ieiri, I., Higuchi, S., and Kohno, K. (2010) Circadian disruption accelerates tumor growth and angio/stromagenesis through a Wnt signaling pathway. *PLoS One* **5,** e15330